

CTH-RF-130

CHALMERS UNIVERSITY OF TECHNOLOGY
DEPARTMENT OF REACTOR PHYSICS



A

29 - 39

ISSN 0281-9775

CTH-RF-130

1997

**Monte Carlo Simulation of
Neutron Transport in a
Homogeneous Reactor with a
Partially Inserted Control Rod**

by

J. K-H. Karlsson and P. Lindén

**Department of Reactor Physics
Chalmers University of Technology
S - 412 96 Göteborg, Sweden
ISSN 0281-9775**

Monte Carlo Simulation of Neutron Transport in a Homogeneous Reactor with a Partially Inserted Control Rod

J. K-H. Karlsson and P. Lindén

Department of Reactor Physics, Chalmers University of Technology
S-412 96 Göteborg, Sweden

Abstract

The neutron transport in a bare, cylindrical and homogeneous reactor, with and without the presence of a central partially inserted control rod, has been simulated by using a Monte Carlo transport code. The behaviour of both the flux and current in this system have been investigated. We have found that the flux and especially the current are strongly affected by the presence of the control rod in its close vicinity. The results indicate the feasibility to identify the position and especially the tip of the rod from the flux and current. Further, the direction to the rod can be found from the current vector. The information content regarding the position of the rod, in both the neutron flux and the current, decays strongly as a function of distance and it is dependent on the size of the rod. In our model, the practical range over which the flux or current can be a useful indicator of the position of the tip of the rod is about 10-15 cm for a rod with a diameter of 2 cm. The practical range for identification of the position of the rod is greater for a rod of larger diameter.

1. Introduction

Recently a proposal was made by Pázsit (Ref. 1) to use the neutron current as well as the flux in core monitoring and diagnostics. Since the neutron current, or the flux gradient in diffusion theory, is angularly dependent (i.e. it is a vector), it contains more information than the scalar neutron flux. The current gives not only the magnitude, but also the direction of neutron transport through a medium. Current detectors do not yet exist, however with today's technology, direction sensitive current or rather flux gradient detectors can be constructed.

To illustrate the potential benefits that current detectors can give in different diagnostic applications, a few model applications have been investigated in Ref. 1. One of these model applications originate in the problem of determining the axial elevation of a control rod in a pressurized water reactor (PWR). The axial elevation or the position of the tip of the control rod is recorded by an electromechanical device, whose precision can decay during operation. In response to this practical problem, a study was made of the possibilities to determine the position of the tip of the rod by using the axial shape of the flux as measured by a traversing in-core detector. This original study was performed and reported in Ref. 2. In the study, a neural network was used for the unfolding the information of the position of the tip of the rod from the axial shape of the flux. The flux shapes used in the training of the network were calculated by the in-core fuel management (ICFM) code SIMULATE. The method was quite successful which was demonstrated in a realistic test case performed by the Ringhals power plant. The method and details regarding its application in the test case are given in Ref. 3.

In the above work it became clear that the measurements had to be taken very close to the control rod in order to be able to reliably determine the rod elevation. The reason was simply that the effect of the absorber on the flux decays quickly with distance (i.e. a few diffusion lengths). Furthermore, a direct visual inspection of the flux does not give a reliable estimate of the rod tip even when the measurements were taken very close to the control rod of interest. Thus, the neural network was a necessary tool to obtain a good estimate of the position of the rod tip. In the light of these results, a more sensitive method that could complement or help improve the present method was sought. Then, the current came up as a candidate for the above purpose.

The neutron current vector is a very sensitive indicator of the presence of a perturbation in the near neutron field, e.g. a boundary or a strong absorber. The current vector can also give the direction and distance to the perturbation. However, a general drawback is that its sensitivity decays quickly and the range over which it is sensitive is only a few diffusion lengths of the medium (i.e. $\sim 10\text{-}15$ cm in light water). In this report we intend to investigate in detail a simple model problem in which we can study the behaviour of the flux and current in relation to the above application of determining control rod elevation in a PWR.

The model consists of a 3-D cylindrical, bare reactor with radius $R = 50$ cm and height $H = 2h = 100$ cm and with an absorber rod of 2 cm diameter present half-way through the reactor from the top to the mid-plane (Fig. 1). The absorber rod is the only inhomogeneity in the model and the reactor medium is otherwise considered homogeneous with constant material properties. The rod is placed in the centre of the cylindrical reactor.

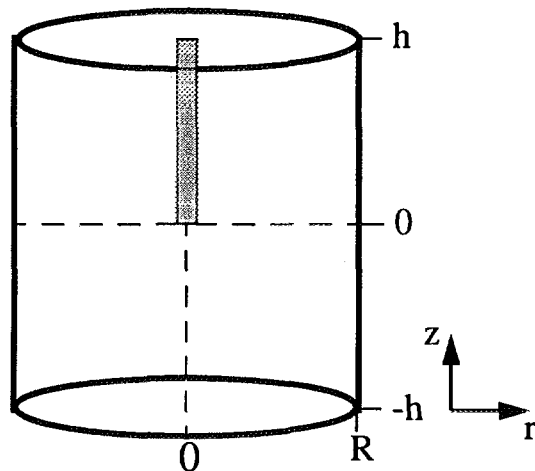


Fig. 1. The cylindrical reactor model with an absorber rod present from the top to the mid-plane of the reactor.

In fact, since the problem is azimuthally symmetric, the flux and current are independent of the azimuthal variable ϕ and the cylindrical reactor model can be reduced from 3-D into a 2-D rectangular reactor model. In the resulting 2-D model semi-analytic solutions of the diffusion equation are possible. These analytic calculations have been performed and will be reported in the near future (Ref. 4). Further, the preliminary results of these analytic calculations of the flux and its gradient have already been compared with the main results of the present work in Ref. 1.

The analytic calculations mentioned above give the one-group diffusion theory solution in the 2-D version of the model. However, the diffusion equation is an approximation of the more general neutron transport equation and it is not strictly valid close to a boundary. For example, in diffusion theory the reactor-vacuum boundary is treated using an assumption of the neutron flux vanishing at one extrapolation distance outside the physical boundary of the reactor. This limitation of diffusion theory applies also to the flux close to an absorber like a control rod. Further, the current is only equal to the flux gradient in case diffusion theory is valid. Thus, to obtain an accurate solution close to the control rod for the flux and more importantly for the current, we prefer a transport theory solution to our problem.

However, the complex form of the neutron transport equation, together with inconvenient boundary conditions, makes it very difficult to solve. In fact, for many reactor physics problems not even a direct numerical solution is possible. An alternative to using the transport equation and still properly model the transport close to boundaries, is to use the Monte Carlo method and follow the actual paths of the neutrons. In this work, we report about the development of a Monte Carlo code for modelling neutron transport in a reactor. Further, we will show the results obtained using the code for the 3-D cylindrical, non-homogeneous reactor model described above.

In a Monte Carlo (MC) transport code a neutron is followed from its birth as a fast neutron through different interactions until it is absorbed or leaks out of the system. The complete life duration of a single neutron from birth to absorption or leakage is hereafter referred to as a neutron history. The macroscopic cross-sections of the different neutron

interactions determine the probability that a specific interaction will occur. Then, a sequence of random numbers is sufficient to determine the history of a single neutron. The different interactions lead to either an end to the neutron history or to the continuation of its life but then with different properties (e.g. different direction). The results of all possible interactions are modelled in the code. For example, if the interaction is a scattering event the neutron remains in the system but its direction of travel and energy is altered. This interaction event is common to both atomic collision cascades and neutrons. However, a special type of interaction which only occurs for neutrons, together with nuclear fuel nuclei, is fission. In a fission event the incoming neutron is absorbed, but as a result of the interaction a number of new fast neutrons are produced. This interaction is of course the reason why there can be a chain reaction at all. A schematic figure of the possible interactions for a neutron is given in Fig. 2.

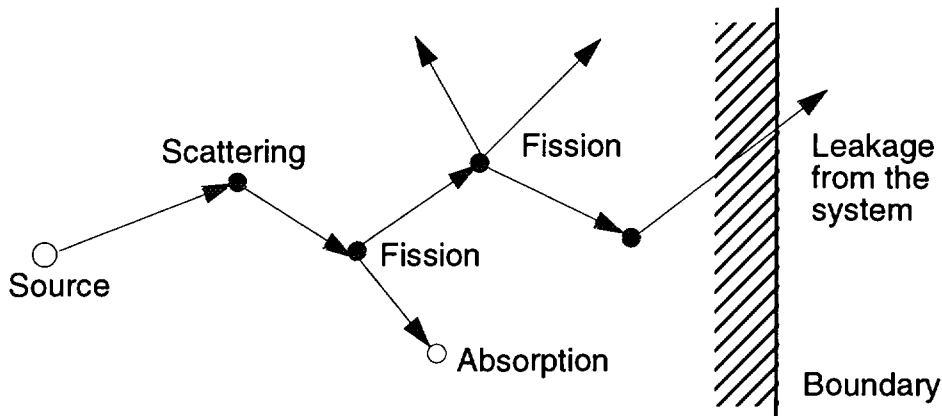


Fig. 2. A schematic view of neutron transport

If there is a balance between the total number of neutrons produced by fission events and the number of neutrons lost from the system, the reactor is critical. A useful concept in this context is the effective multiplication factor, k_{eff} , defined as the fraction of the number of neutrons produced in the system and the total number of neutrons absorbed in and leaked out of the system. Consequently, k_{eff} is equal to unity for a critical system and a slight change from unity will cause the neutron flux to grow (i.e. $k_{eff} > 1$) or decay (i.e. $k_{eff} < 1$) exponentially.

This report is organized as follows. Section 2 contains a description of the MC code. The results of the simulations performed for the previously described model problem are given in Section 3. Finally, the results are discussed in Section 4. Further, it should be stated that apart from the above given motivation for this work, we have also performed this work as part of the course “Computational Physics” and in order to learn the MC method.

2. Description of the Monte Carlo code

The above described transport process was turned into a Monte Carlo code and run on a SPARC Server 20. The implementation was greatly simplified compared to realistic problems, due to different approximations: The reactor has no reflector, and it is a homogeneous mixture of ordinary water and uranium fuel. The concentration of fuel is set to 25 (g fuel)/(kg moderator). The fuel is assumed to be uranium, consisting of the two isotopes ^{238}U and ^{235}U , where the only fissile isotope is ^{235}U . The enrichment fraction, i.e. the fraction of ^{235}U in the

fuel, is a parameter that can be used to tune the reactor to criticality. The critical enrichment fraction for the case of no rod present is approximately 5.2%.

The neutrons are assumed to be born thermal, i.e. there is no energy dependence. In reality the neutrons are born with high energies and then slowed down by scatterings until they reach thermal equilibrium with the medium. At thermal energies, the neutrons diffuse until they are absorbed or lost from the system. The cross-sections, densities, atomic weights and other physical properties have been gathered from tabulated values. The cross sections were taken from Ref. 5. Further the introduced control rod with diameter 2 cm is positioned in the radial centre and from the top to the mid-plane (i.e. $z = 0$) of the reactor. The rod is assumed to absorb every neutron that hits its surface and hence no neutrons return from the rod, which is not true for a realistic control rod.

The actual simulation begins by sampling the positions and direction vectors for 10,000 neutrons inside the reactor. The initial positions of the neutrons are sampled according to the distribution obtained from the solution of the diffusion equation with no rod present Eq. (1).

$$\phi(r, z) = C \cdot J_0(\lambda_1 r) \cos(\lambda_2 z) \quad (1)$$

where C is a normalization constant, $\lambda_1 = 2.405/R$, R is the extrapolated radius, $\lambda_2 = \pi/H$ and H is the extrapolated height of the cylinder. The Metropolis algorithm, Ref. 6, is used in the sampling of the positions of the neutrons according to the above distribution, while the initial directions of travel are sampled isotropically in space.

The generated initial positions and directions of travel are saved in an account for the current generation of neutrons in a bank, i.e. an array. The history of a single neutron is then started by withdrawing its initial position and direction of travel from the bank. The single neutron is then considered thermal at its initial position. The probabilities for interaction are now used to sample a random penetration depth. The penetration depth is the distance the neutron travels before it undergoes an interaction of any kind. The penetration distance, l , is sampled according to the exponential distribution Eq. (2), where ξ is a uniformly distributed random number on $[0,1]$ and Σ_{tot} is the total macroscopic cross-section.

$$l = -\frac{\ln(\xi)}{\Sigma_{tot}} \quad (2)$$

The neutron is followed as it travels the penetration distance in its initial direction of travel. To count the neutron flux and current density, a 3 dimensional cartesian mesh has been constructed. This construction yields that the volume of the cartesian meshes positioned at the radial boundary of the cylinder varies and that effect is considered in the calculations.

The “track length” or “path length” estimator has been used to estimate the scalar flux in the mesh volumes. The average scalar flux $\bar{\phi}$ in a volume V , may be defined as the total track length traversed by all neutrons per unit volume per unit time, Ref. 7. If p_n is the path length in V of the n th neutron, the average scalar flux can then be estimated as

$$\bar{\phi} = \frac{1}{V} \cdot \frac{1}{N} \cdot \sum_{i=1}^N p_n \quad (3)$$

where N is the total number of neutrons in the simulation. To get an estimate of the error in the scalar flux the following relationship has been used:

$$\Delta\phi = \frac{1}{V} \cdot \sqrt{\frac{N}{N-1} \cdot \left(\frac{1}{N} \cdot \sum_{n=1}^N (p_n)^2 - \bar{p}^2 \right)}. \quad (4)$$

Whenever a neutron travels through the mesh volumes the total path lengths in the volumes are stored together with the square of the path lengths and after all neutrons have been launched, the scalar flux and its error in the mesh volumes are calculated.

Since the neutron current density is a vector, the code needs to keep track of the direction of travel of the neutron through the mesh volumes. Two counters for each coordinate direction are used to determine the neutron current density. One counter is increased by one when a neutron passes the mid-plane of the volume mesh in the positive coordinate direction and the other counter is increased by one when the neutron travels in the opposite direction. Thus, a component of the neutron current density is obtained for each coordinate direction by the difference of the two counter values.

Because the neutron current requires a considerably larger number of neutron histories in order to obtain good statistical accuracy, the cylindrical symmetry was also used to count the neutrons moving in and out of a shell of a much larger radius than the volume mesh discussed previously. In this case, the radial component of the neutron current is determined. For the axial component the same method is used for axially spaced planes. Thus, the components of the neutron current were calculated by averaging over many neutrons and a reasonable accuracy was obtained. To estimate the accuracy of the neutron current, batches of neutron histories are run and the neutron current for each batch is determined. The mean neutron current from these batches is then estimated and an associated standard deviation is also calculated. The standard deviation of the mean neutron current is taken as a measure of the accuracy.

The next step is to treat the different interactions that can occur when the neutron reaches the end point of the penetration distance. The type of reaction is sampled by picking a uniform random number on $[0,1]$ and comparing it with the probabilities for the different interactions. Scattering will then occur in ~96% of all cases. The scattering interaction is modelled by assuming it to be isotropic in the laboratory system. This is reasonable at thermal energies and heavy elements, but not at higher ones and for water. Thus, at the scattering interaction a new direction of travel is sampled for the neutron and then a new penetration distance to the next interaction. The neutron continues on its new path.

However, the neutron may undergo absorption or can leak out from the system, which is just the removal of the neutron from the reactor. In such a case the current neutron is lost and thus the position and direction of travel of a new neutron is withdrawn from the bank, and a new

history is started in the same way as previously described. If the neutron hits the control rod, it is absorbed in the same way as above.

In about 2% of all cases a fission reaction occurs. At the fission interaction the current neutron is absorbed, but as a result of the fission event a number of new independent neutrons are born. The number of new neutrons varies, but two or three are the most common values and the mean is 2.42. The number of new neutrons, two or three, is sampled from a uniform random deviate, with such a probability that the average becomes 2.42. The newborn neutrons are fast and they quickly lose energy through scatterings. However, the slowing down is a complicated process to model and more or less unnecessary for the scope of this project. In order to take the slowing down into account in a very simple manner, a random distance is sampled from a Gaussian distribution. The variance used is a tabulated material property (i.e. age) of the moderator. Thus, each newborn neutron is given an initial position at a random slowing down distance from the original position of the fission event. Therefore, they are effectively born at thermal energies. Further, there is a probability for a newborn neutron to be absorbed during the slowing down process. An estimate of the probability for not being absorbed is made. This probability is then used to determine if the neutron is absorbed during slowing down or not. Then, for each surviving neutron a new direction of travel is sampled of an isotropic distribution. Finally, the information on positions and directions of travel for the new neutrons is saved in the bank in a new account for the next generation of neutrons. Since the incoming neutron was absorbed, the position and direction of travel for a new neutron is withdrawn from the bank, but of course from the account of the current generation.

When the account for the current generation of neutrons is empty, the accounts are swapped and the next generation becomes the current generation instead. A new initial position and direction of travel is taken from the account and a new generation of neutron histories begins. The number of neutrons in the next generation is equal to the number of surviving neutrons born in fission reactions, whereas the neutrons in the previous generation disappear by leakage, absorption and fission. Each time the generations are swapped, the effective multiplication factor k_{eff} is calculated and written to a log file. k_{eff} is equal to the number of neutrons in the new generation divided by the number of neutrons in the previous generation. Thus, one can follow how the simulation develops. If the reactor is stationary, i.e. critical, and only normal statistical fluctuations occur, the whole bank is never completely emptied and the simulation may continue forever. If more neutrons are created than absorbed, the bank will eventually overflow and the simulation will stop. This is what happens if the reactor is supercritical. If, instead, fewer neutrons are created than absorbed, the bank will end up completely bankrupt and the simulation will stop as well. This is the subcritical state for a reactor. In case the reactor is close to critical, the simulation is stopped manually after a default number of generations, usually several thousands. In reality, the time between each generation of neutrons corresponds to the prompt neutron generation time (i.e. ~1 ms). It is worth to note that our code does not include any delayed neutrons, only prompt ones.

The statistics gets better and better for each generation. However, to obtain good statistics several thousands of generations or several tens of millions of individual neutron histories are needed. The results shown in Section 3 have the best statistics that we obtained from the performed simulations.

3. Results

As the simulation proceeds, a visual inspection of how the chain of calculated k_{eff} values develops is performed. The first few values of k_{eff} indicate the occurrence of a transient in the number of neutrons during the first few generations. This is due to the initial distribution of the positions of the first generation of neutrons. This distribution is the solution to the diffusion equation for a cylindrical reactor without a control rod. Since diffusion theory is only an approximation, the simulation will immediately tend towards the true transport behaviour. However, the diffusion approximation gives a relatively good description of the situation at hand, only a few generations are needed to reach true transport equilibrium. Assuming that we are close enough to the critical reactor, only natural statistical fluctuations occurs in the value of k_{eff} after the first few generations.

Two simulations, one with and one without the presence of the control rod, have been performed. The neutron flux and current have been calculated in a large number of positions for each simulation. The results for both the flux and current are presented below.

3.1 The neutron flux

In the case of the unperturbed reactor, we can compare the results of the simulation with the solution of the diffusion equation Eq. (1) with extrapolated boundaries. Since diffusion theory is a relatively good approximation of the actual transport in large diffusive systems, the MC results are expected to agree quite well with the diffusion solution. The neutron flux obtained for the unperturbed system and the diffusion solution Eq. (1) are shown together in Fig. 3a. Further, the constant C and the extrapolated boundaries R and H in Eq. (1) have been fitted to the results of the MC calculation.

As can be seen in Fig. 3a, the neutron flux obtained from the calculation corresponds quite well to the shape of the diffusion solution. The error bars shown in the figure indicate the error corresponding to one standard deviation of the calculated value for the flux at that position.

Regarding boundary conditions in reality, the neutrons that leave a system are lost and does not re-enter the system. Thus, the proper boundary condition in transport theory is that there should be an outgoing flux of neutrons, i.e. positive neutron current in e.g. the radial direction, but no incoming flux. In diffusion theory this cannot be taken into account and the boundary condition is instead taken to be zero neutron flux at the so called extrapolated boundary. This difference shows that diffusion theory cannot be valid close to boundaries, as have been previously mentioned. The performed calculations give non-zero values for the neutron flux at the physical boundaries, which is in qualitative agreement with transport theory.

In the simple MC code described in Section 2 we assumed isotropic scattering in the laboratory system of the neutrons. This is strictly not true, especially not for hydrogen atoms. This does not affect the general conclusions of this report. However, it does affect somewhat the values of both the diffusion coefficient and the diffusion length. Further, the distance outside the boundary where the solution to the diffusion equation should become zero, in order to follow the transport solution as closely as possible inside the core, is called the extrapolation distance d . Assuming completely isotropic scattering in the simulation, this distance can be found as $d = 0.71/\Sigma_s \approx 0.5$ cm, where Σ_s is the total macroscopic scattering cross-section. The

extrapolated distance is found from our calculations by extrapolating the flux to zero outside the boundary (see Fig. 3b). The result is ~ 0.4 cm, which agrees well with the calculated value above.

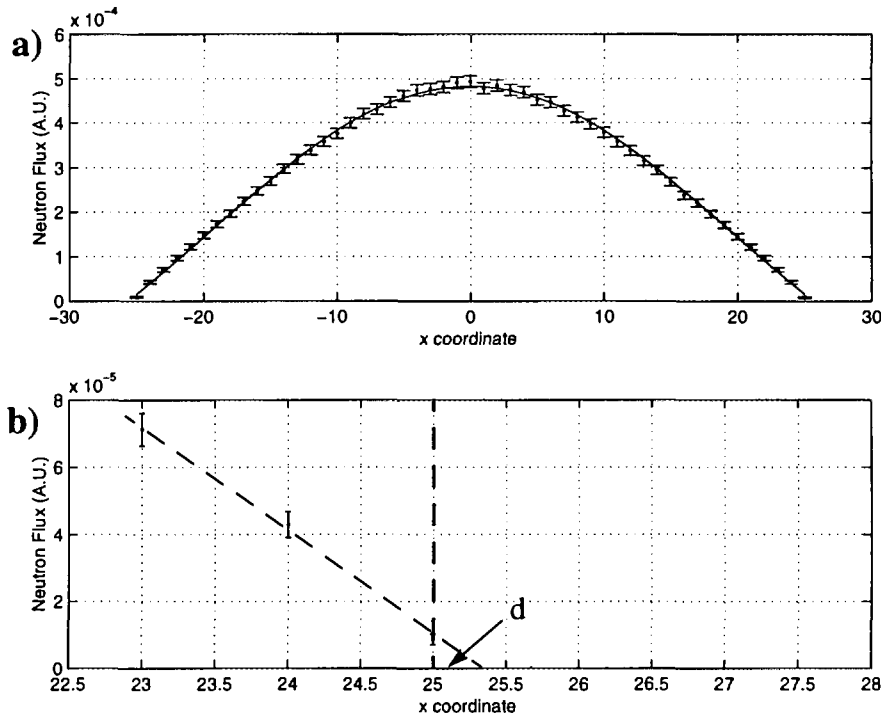


Fig. 3. Figure a) shows the neutron flux with error bars along the diameter (called the x-coordinate [cm]) at the axial centre of the reactor. Figure b) shows three values of the flux close to the boundary connected with a line, which indicates the extrapolation distance.

In Fig. 4 the neutron flux is shown along the diameter of the reactor at the axial centre of the reactor (i.e. $z = 0$) for the perturbed reactor with the rod present (i.e. the dash-dotted line) and the unperturbed one (solid line). Due to the presence of the control rod, whose position is indicated in the figure, the neutron flux is strongly suppressed close to the rod (see the dash-dotted line in Fig. 4). However, with the exception of the region in the vicinity of the rod, the overall behaviour is similar to the case with no rod present (i.e. the solid line). Actually, already at this point we get an indication of the distance over which a strong perturbation affects the flux. It is seen in Fig. 4 that the cases with the rod and the one without the rod are practically the same for $|x| > 10$ cm corresponding to ~ 4 diffusion lengths. However, if we would shrink the rod to a δ -function, practically no neutrons would hit the rod and thus no neutrons would be absorbed. It is clear that the perturbation in the flux and current depends not only on the distance from the rod but also on the size of the rod. Thus, the larger the diameter of the control rod the greater the distance over which it will perturb the flux and current. The dependence of the critical flux and buckling on the rod size is analysed in detail in Ref. 8. For our rod with 2 cm diameter the information content (i.e. position and direction to the rod), which is carried by the distortion of the flux around the rod, decays fast with distance and it practically vanishes for distances larger than about 10 cm.

Fig. 5 shows the flux as a function of axial elevation for the case with the rod present (dash-dotted line) and without the rod present (solid line) for two distances from the centre of

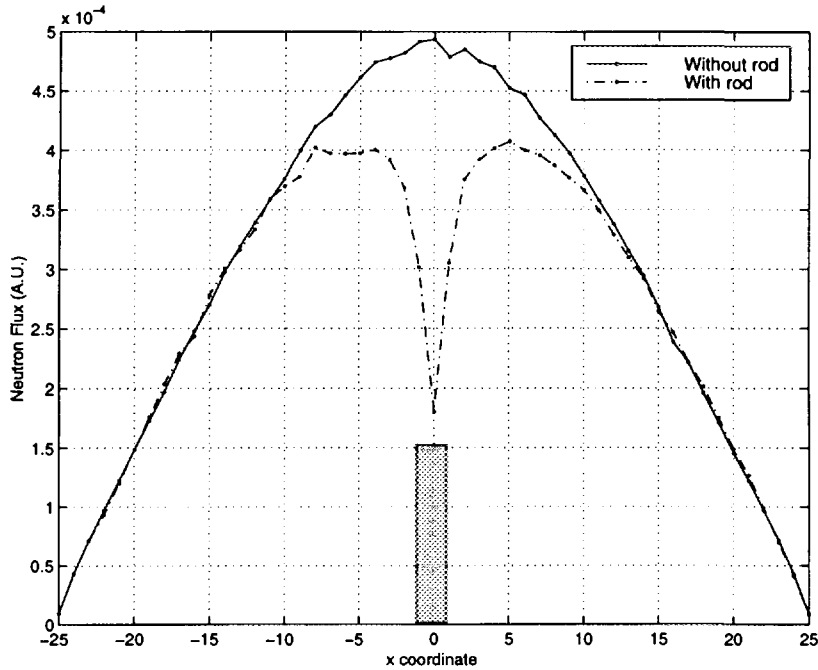


Fig. 4. The neutron flux along the diameter of the reactor for the two cases with the rod present (dash-dotted line) and without the rod present (solid line).

the reactor, a) 2 cm and b) 10 cm. The rod extends from the top (i.e. $z = 50$ cm) to the centre of the reactor (i.e. $z = 0$ cm), which is shown by the bar on the l.h.s. in the figure.

The solution of the diffusion equation without rod as a function of axial position is a cosine as seen in Eq. (1). As in Fig. 3 the unperturbed flux in Fig. 5 closely follows this solution of the diffusion equation. Further, a comparison between the two curves in Fig. 5a shows that the neutron flux is strongly affected by the presence of the rod. Only a few cm above $z = 0$, the amplitude of the flux is strongly suppressed by the rod, while its shape follows the cosine profile of a homogeneous core. Right at the tip of the rod, the neutron flux strongly deviates from the diffusion solution. Here, the flux increases with a large gradient for about 4 cm around the tip of the rod and then it follows the cosine profile of a homogeneous core again, but now with a similar amplitude as the unperturbed flux.

In diffusion theory the neutron current is proportional to the gradient of the neutron flux and from this fact it can be surmised that the current will show an even stronger deviation than the neutron flux at the tip of the rod. It is clear from Fig. 5a that close to the rod, the axial position of the rod tip can be determined from the behaviour of the flux itself with good accuracy by a simple visual inspection. However, Fig. 5b shows that only a few centimetres further away from the rod, the task to determine the position of the rod tip becomes much harder. In this case the current can be a better tool to indicate the position of the rod tip.

The 2-D neutron flux at the mid-plane of the reactor (i.e. at $z = 0$) is shown in Fig. 6. This result is obtained for the unperturbed reactor, i.e. without the presence of the control rod. The previously mentioned cylindrical symmetry of the neutron flux is obvious. The maximum flux is found in the centre of the reactor and hence the rod has the strongest possible effect at that location. To compensate the strength of the rod, the simulation is run with a larger enrichment fraction when the rod is present. The absorption strength of the rod corresponds to a subcritical reactivity value of ~ 300 pcm.

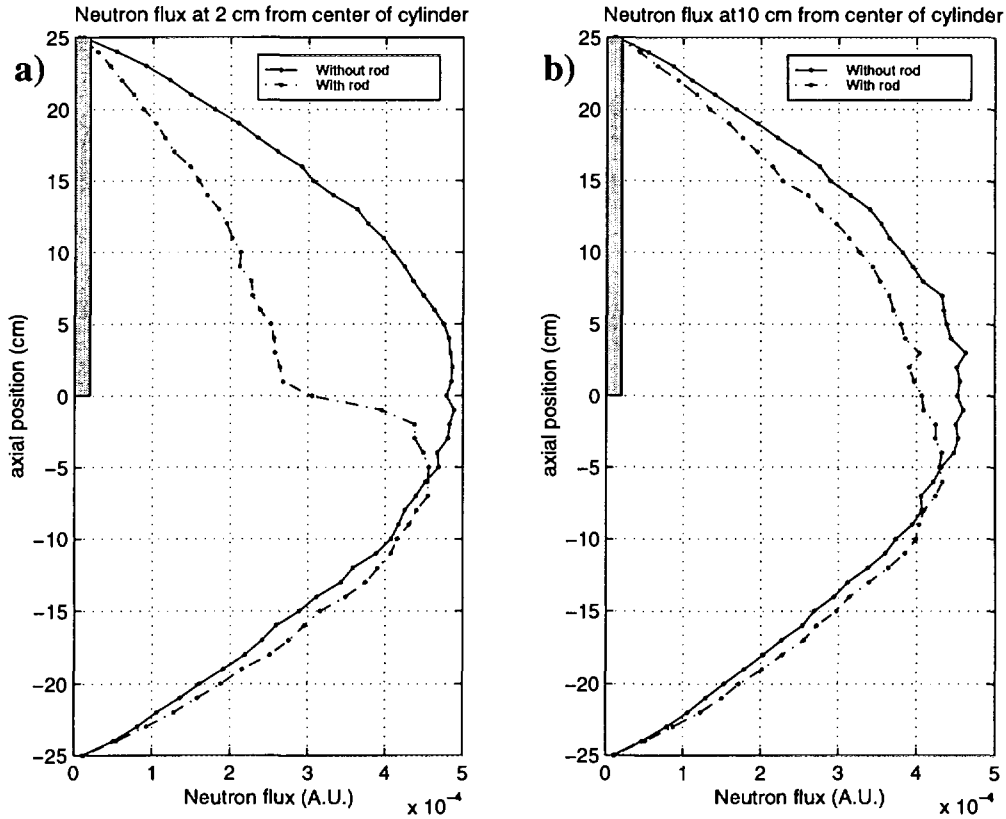


Fig. 5. The figure shows the flux as a function of axial elevation for the case with the rod present (dash-dotted line) and without the rod present (solid line) and also for two distances from the centre of the reactor, i.e. a) 2 cm and b) 10 cm.

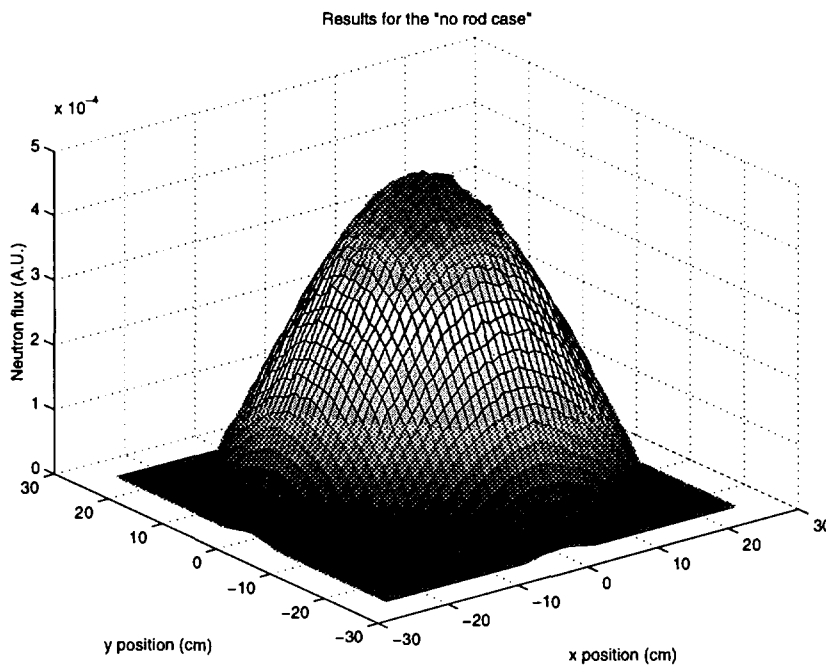


Fig. 6. The 2-D neutron flux for the unperturbed system.

The model problem of a partially inserted control rod has also been studied using an ICFM code system (Refs. 2 and 3). The code consists of two parts, called CASMO and SIMULATE. CASMO is used to solve the transport equation for each unique fuel element and its output is used in SIMULATE to solve the two-group diffusion equation for a full core. The SIMULATE results for the neutron flux in an unperturbed fuel element (solid line) and the same element containing a control (dashed line) rod are shown in Fig. 7. The unperturbed flux in Fig. 7 is not a cosine like in our unperturbed system above, since the core model used to calculate the fluxes in Fig. 7 is heterogeneous. This is also the reason for the wiggles on the unperturbed flux and they correspond to the presence of the spacer grids on the fuel elements. Further, the neutron flux for the case with the rod present (Fig. 7) essentially exhibits the same qualitative behaviour as we observed in the MC calculations (c.f. Fig. 5). This commercial code is very accurate and thus it gives strong qualitative support to our results. However, a quantitative comparison is not possible and the main reason is that our system is assumed to be homogeneous, while a realistic reactor core as calculated by SIMULATE is heterogeneous.

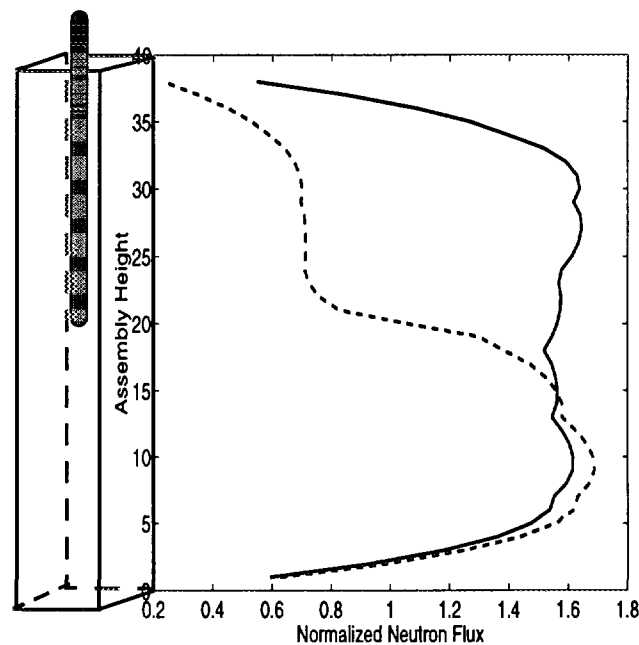


Fig. 7. The axial neutron flux inside a fuel element. The solid curve is the neutron flux without the rod present. The dashed curve shows the distortion of the neutron flux caused by the presence of the rod.

3.2 The neutron current

The neutron current density J is a vector and in diffusion theory it is directly proportional to the negative neutron flux gradient as

$$J = -D\nabla\phi \quad (5)$$

Thus, for the unperturbed case the qualitative shape of the current is easily obtained from the negative flux gradient of the solution to the diffusion equation. Therefore, in the centre of the reactor the current should be zero. Due to the azimuthal symmetry in both cases calculated in this report, the current is also zero in the azimuthal direction and the current has only r and z

components. For the unperturbed case, the radial component of the current should increase in the outwards radial direction to reach its maximum at the boundary of the reactor. The z-component of the current density displays the same behaviour along the axial elevation of the reactor. These features of the current vector in the unperturbed system are displayed in Fig. 8. The arrows in Fig. 8 show both the relative magnitude and the direction of the current vector as a function of position.

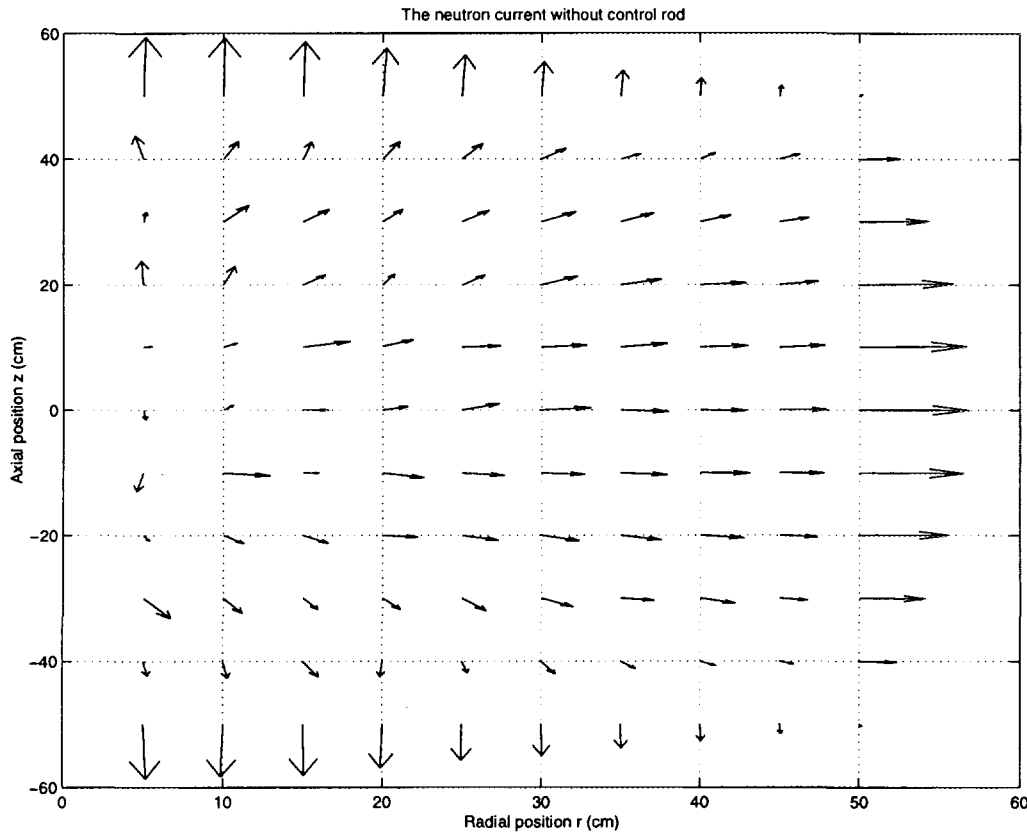


Fig. 8. The neutron current as a function of position in r, z geometry. The arrows show both the relative magnitude and the direction of the current vector as a function of position.

Fig. 9a shows the current vector in the unperturbed system for radii between $r = 0$ and $r = 10$ cm. For comparison, a similar figure of the current for the case with the rod present is shown Fig. 9b. A comparison of the figures immediately indicates the presence and position of the rod in Fig. 9b. In Fig. 9a the z -component of the current density vector is directed outward everywhere, except in the centre of the reactor where it is practically zero. For the case with the control rod present, the large magnitude and direction of the current close to the rod in Fig. 9b shows the position and direction to the rod and especially its tip.

In Fig. 10 the radial component of the current is shown as a function of axial position, for three different radii and for both the unperturbed (Fig. 10a) and the perturbed system (Fig. 10b), respectively. Note that in this figure a negative value of the radial component of the current corresponds to the inward direction and a positive value means an outgoing current, respectively. Further, the position of the rod is given as a bar in Fig. 10b. In this figure the errors associated with the calculated values of the current are also given. The errors are large where

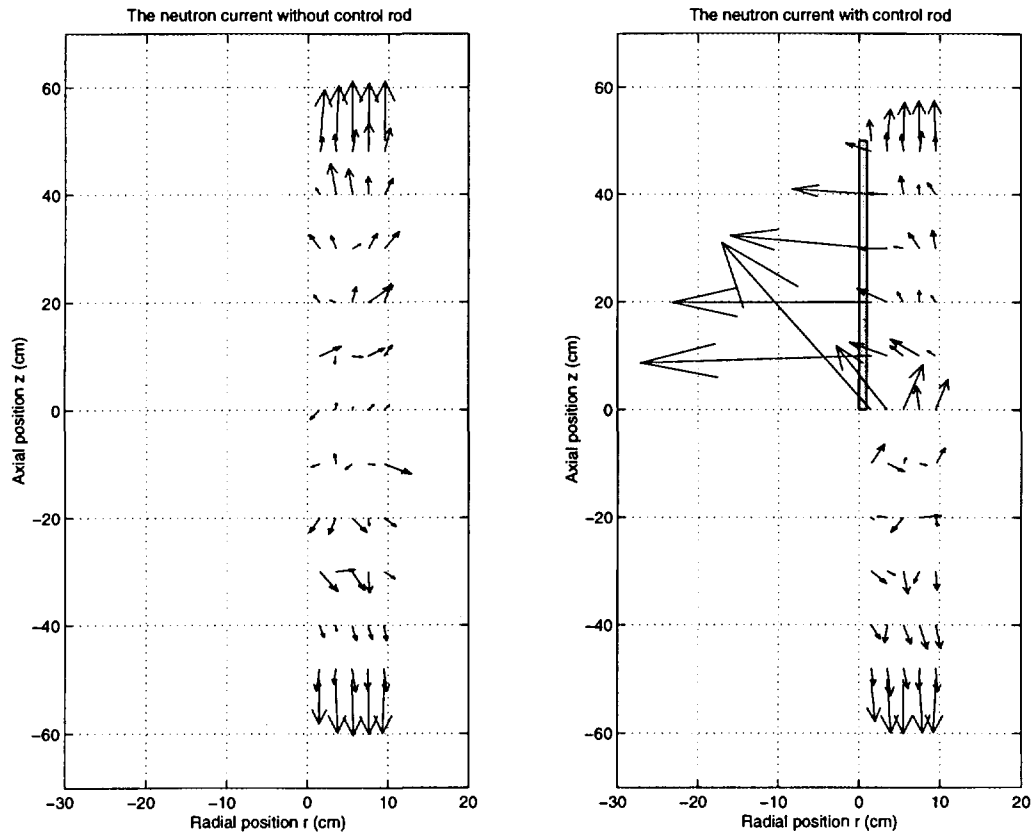


Fig. 9. The neutron current vector as a function of position for a) the unperturbed reactor and b) the reactor with the rod present.

the net current is close to zero, e.g. at the centre of the unperturbed reactor. At positions where the net current is significantly different from zero, the errors are relatively small.

The large magnitude of the current close to the rod, which is shown in Fig. 10b, suggests that if a current density detector existed, it would give the position of the tip of the rod within a few centimetres or less. However, the influence of the rod on the neutron current decays with increasing distance from the rod, much in the same way as previously described for the neutron flux. At a distance corresponding to ~ 4 diffusion lengths or 10 cm from the rod it is very difficult to notice any depression or direction towards the rod in the radial component. Thus, the practical range over which the flux or current can be a useful indicator of the position of the tip of the rod is about 10-15 cm for our rod of 2 cm diameter.

4. Conclusions

The problem presented in Section 1 has been solved by using a Monte Carlo code. The results are illustrative and give a good qualitative understanding of the behaviour of the flux and current in this system.

The qualitative results both for the neutron flux and the neutron current density agree with their expected behaviour. Despite its small diameter, the control rod is rather strong and its effect on the neutron flux is clearly illustrated in the results. Further, if we would shrink the rod to a δ -function, practically no neutrons would hit the rod and thus no neutrons would be absorbed. Thus, the perturbation in the flux and current depends on the size of the rod. For the

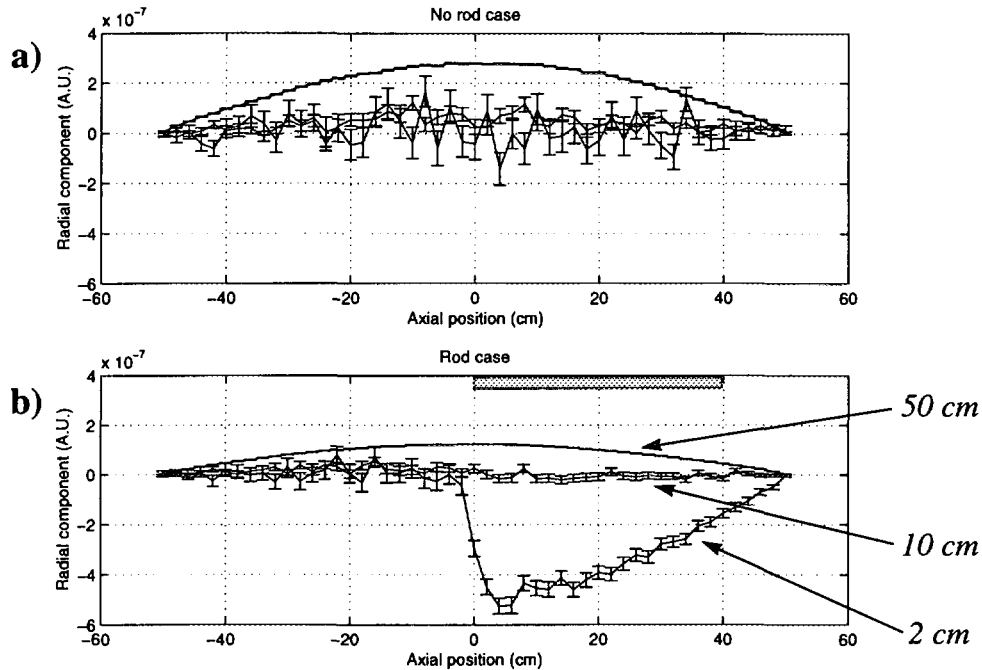


Fig. 10. The neutron current with error bars as a function of axial position, for three different radial positions from the centre of the reactor and for a) the unperturbed reactor and b) the reactor with the rod present.

present model, where the rod has a diameter of 2 cm, the shape of the neutron flux is almost undisturbed ~ 10 cm (i.e. ~ 4 diffusion lengths) from the rod. These results show that the rate of decay of the neutron flux, as one moves away from a rod of 2 cm diameter, is rather strong. Thus, in our model the practical range over which the flux or current can be a useful indicator of the position of the tip of the rod is about 10-15 cm. Further, the practical range for identification of the position of the rod is greater for a rod of larger diameter.

The neutron current density behaves simply like the gradient of the flux when no rod is present. However, the current is even stronger affected by the presence of the rod than the neutron flux. The decay of the distortion of the current density, as one moves away from the rod, is similar to the that of the flux. Further, the results show that in the vicinity of the rod the direction of the current is a valuable and good indicator of the direction to the rod and especially to its tip. The results presented in this report indicate what to expect, if a possible current density detector can be manufactured and tested close to a control rod.

Acknowledgements

The authors are indebted to Dr. N. Garis for his kind permission to use Fig. 7. In addition we would like to thank Dr. R. Chakarova for introducing us to the Monte-Carlo method.

References

- [1] Pázsit I. (1997), *On the Possible Use of the Neutron Current in Core Monitoring and Noise Diagnostics*, *Ann. nucl. Energy* **24**, 1257
- [2] Garis N. S., E. Temesvári and I. Pázsit (1996), *The feasibility of using neural networks for determination of control rod elevation in a PWR*, Department of Reactor Physics report CTH-RF-117
- [3] Garis N. S., Pázsit I., Sandberg U. and Andersson T. (1998) *Determination of PWR control rod position by core physics and neural network methods*. To appear in *Nucl. Technology*
- [4] Karlsson J. K-H. and Pázsit I. (1998), *An analytically solvable axially non-homogeneous reactor model. I. General solutions*, Submitted to *Ann. nucl. Energy*
- [5] Mughabghab S. F., Divadeenam M. and Holden N. E. (1981), *Neutron Cross Sections, Volume 1, Part A*, Academic Press, Inc.
- [6] Kalos M. H. and Whitlock P. A. (1986), *Monte Carlo Methods, Volume I: Basics*, John Wiley & Sons, Inc.
- [7] Lewis E. E. and Miller, Jr. W. F. (1984), *Computational methods of neutron transport*, John Wiley & Sons, Inc.
- [8] Pázsit I. (1994), *Comment on the Modelling of Thin Absorbers via δ -functions*. *Nucl. Sci. Engng.* **116**, 223